

Electronic Supplementary Material (ESI) for Nanoscale.  
This journal is © The Royal Society of Chemistry 2020

## **Supporting Information**

# **Metasurface-Enabled Broadband Beam Splitters Integrated with Quarter-Wave Plate Functionality**

Fei Ding,<sup>\*</sup> Rucha Deshpande, Chao Meng, and Sergey I. Bozhevolnyi

Centre for Nano Optics, University of Southern Denmark, Campusvej 55, DK-5230 Odense,  
Denmark

<sup>\*</sup>To whom correspondence should be addressed. Email address: feid@mci.sdu.dk.

## Section S1. The beam splitter composed of the four-element-based supercell

As described in the main text, the split angle is determined by the generalized Snell's law for normal incident light:  $\theta = \sin^{-1}(\lambda/(np))$ , where  $\lambda$  is the wavelength in free space and  $n$  is the number of elements compose a supercell. To make sure the incident light can be reflected to the propagating wave, the periodicity of the supercell should be larger than the wavelength (i.e.,  $np > \lambda$ ). Otherwise, the incident light will become the surface wave. Therefore,  $n$  can take an arbitrary even integer larger than 2. If  $n$  becomes larger, the split angle is getting smaller.

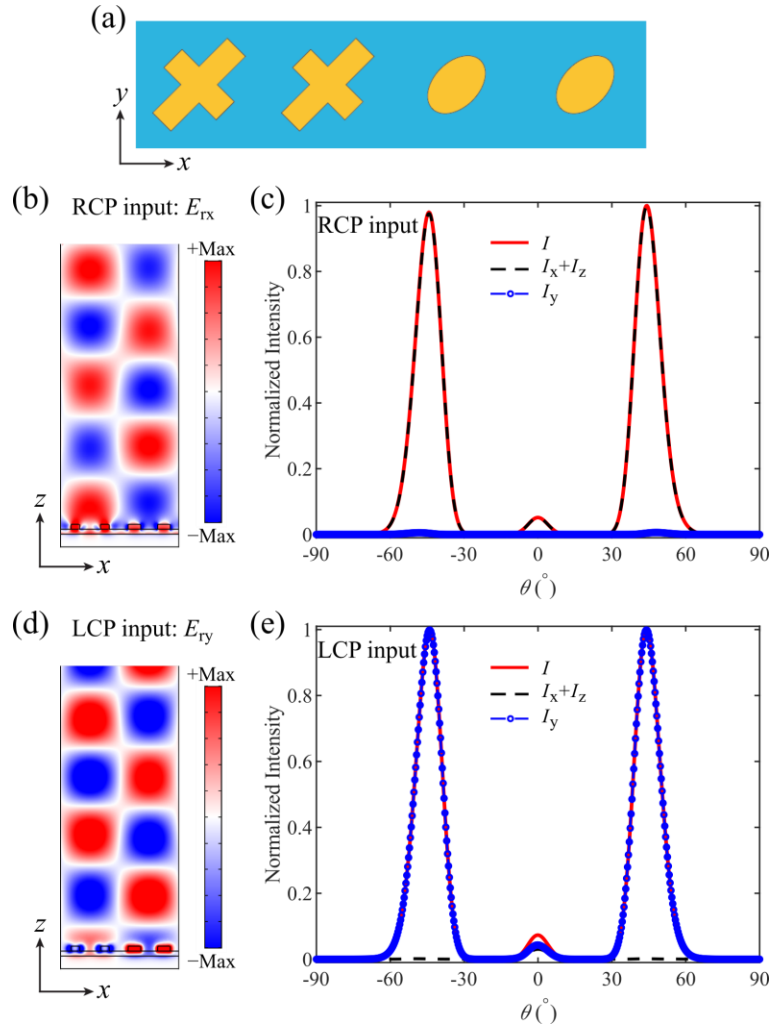


**Fig. S1** (a) Schematic of the metasurface supercell consisting of 4 elements. (b,c) Simulated results of the beam splitter for RCP input, displaying (b) the  $x$ -component of the reflected E-field ( $E_{rx}$ ) and (c) the normalized 2D scattering pattern of different components ( $xoz$ -plane). (d,e) Simulated results of the beam splitter for LCP input, displaying (d) the  $y$ -component of the reflected E-field ( $E_{ry}$ ) and (e) the normalized 2D scattering pattern for different components ( $xoz$ -plane).

To validate the versatility of our metasurface-enabled beam splitter, here we analyze another design with 4 elements constructing the metasurface supercell, as shown in Fig. S1(a). Similarly, the electric field distributions exhibit the interferences between multiple reflection beams in different directions [Fig. S1(b) and S1(d)]. Also, the split beams ( $\pm 1$  diffraction orders) in reflection become linearly polarized, whose angles of linear polarization are determined by the spins of the incident light [Fig. S1(c) and S1(e)]. For instance, the LCP incident light is split into *s*-polarized beams only containing  $E_y$  components, whereas other components are almost totally suppressed [Fig. S1(e)]. From the far-field distributions, the split angle is estimated to be  $\pm 43.92^\circ$ , consistent with the theoretical values of  $\pm 45.1^\circ$ . Besides the design wavelength of  $\lambda = 850$  nm, the four-element-based beam splitter shows excellent performance of beam splitting and polarization conversion in the wavelength range of 750 – 950 nm, shown in Fig. S2.

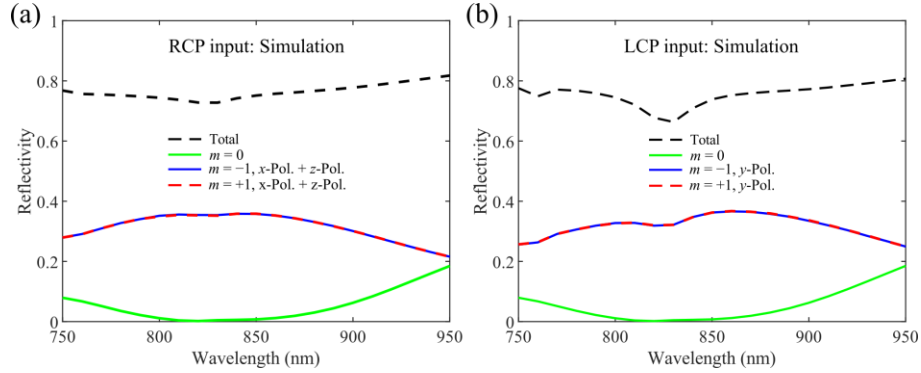


**Fig. S2** Simulated amount of light reflected into the lowest diffraction orders  $m$  and polarization bases as a function of wavelength when the (a) RCP and (b) LCP light is normally incident on the supercell composed of 4 elements.

**Section S2. Theoretical performance of the metasurface-enabled broadband optical beam splitter at wavelengths of  $\lambda = 800$  and  $900$  nm**

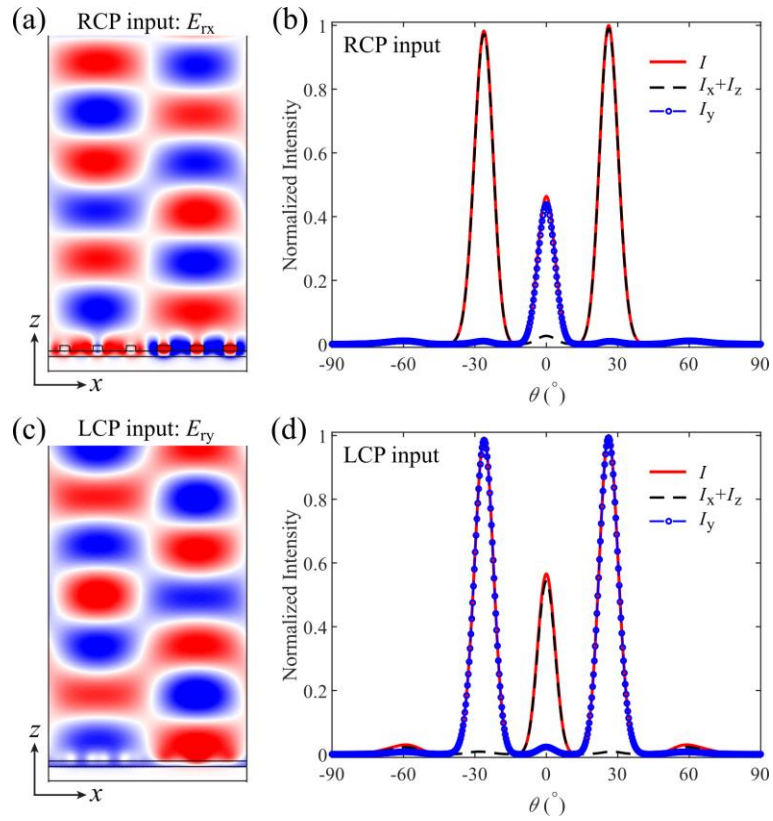


**Fig. S3** Theoretical performance of the metasurface-enabled broadband optical beam splitter at  $\lambda = 800$  nm. a,b) Simulated results of the beam splitter for RCP input, displaying a) the  $x$ -component of the reflected E-field ( $E_{rx}$ ) and b) the normalized 2D scattering pattern for different components ( $xoz$ -plane). c,d) Simulated results of the beam splitter for LCP input, displaying c) the  $y$ -component of the reflected E-field ( $E_{ry}$ ) and d) the normalized 2D scattering pattern for different components ( $xoz$ -plane).

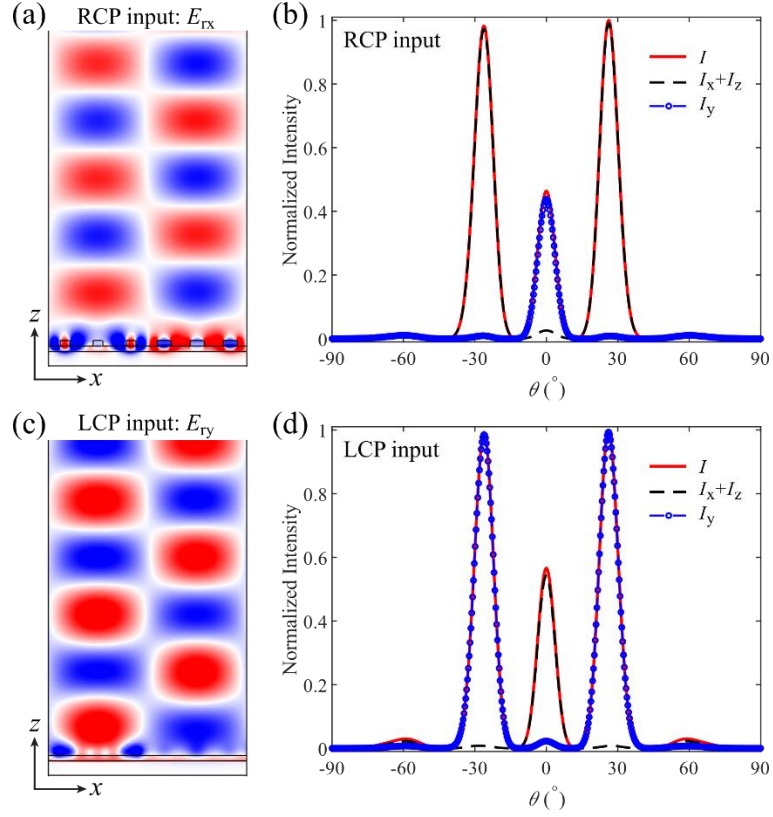


**Fig. S4** Theoretical performance of the metasurface-enabled broadband optical beam splitter at  $\lambda = 900$  nm. a,b) Simulated results of the beam splitter for RCP input, displaying a) the  $x$ -component of the reflected E-field ( $E_{rx}$ ) and b) the normalized 2D scattering pattern for different components ( $xoz$ -plane). c,d) Simulated results of the beam splitter for LCP input, displaying c) the  $y$ -component of the reflected E-field ( $E_{ry}$ ) and d) the normalized 2D scattering pattern for different components ( $xoz$ -plane).

### Section S3. Optical setup for characterization

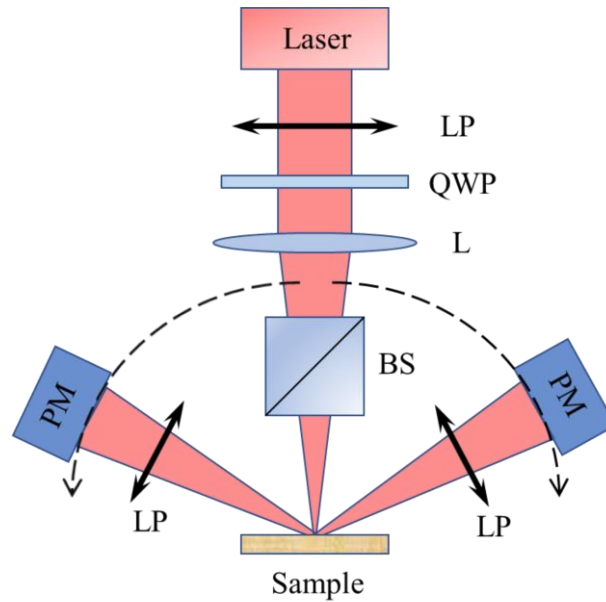


**Fig. S5** The experimental setup for optical characterization of dual-band metasurface. LP: linear polarizer, QWP: quarter-wave plate, L: focusing lens, BS: beams splitter, PM: power meter. The light diffracted at different diffraction orders ( $m = +1, 0, -1$ ) is measured and normalized with the incident measured light to obtain reflectivity. The polarization states are verified by inserted a linear polarization analyzer in front of the power meter.